

This is a self-archived version of an original article. This version may differ from the original in pagination and typographic details.

Author(s): Mahambo, Emanuel T.; Uwamariya, Colores; Miah, Masum; Clementino, Leandro da Costa; Alvarez, Luis Carlos Salazar; Di Santo Meztler, Gabriela Paula; Trybala, Edward; Said, Joanna; Wieske, Lianne H. E.; Ward, Jas S.; Rissanen, Kari; Munissi, Joan J. E.; Costa, Fabio T. M.; Sunnerhagen, Per; Bergström, Tomas; Nyandoro, Stephen S.; Erdelyi, Mate

Title: Crotofolane Diterpenoids and Other Constituents Isolated from *Croton kilwae*

Year: 2023

Version: Published version

Copyright: © 2023 the Authors

Rights: CC BY 4.0

Rights url: <https://creativecommons.org/licenses/by/4.0/>

Please cite the original version:

Mahambo, E. T., Uwamariya, C., Miah, M., Clementino, L. D. C., Alvarez, L. C. S., Di Santo Meztler, G. P., Trybala, E., Said, J., Wieske, L. H. E., Ward, J. S., Rissanen, K., Munissi, J. J. E., Costa, F. T. M., Sunnerhagen, P., Bergström, T., Nyandoro, S. S., & Erdelyi, M. (2023). Crotofolane Diterpenoids and Other Constituents Isolated from *Croton kilwae*. *Journal of Natural Products*, 86(2), 380-389. <https://doi.org/10.1021/acs.jnatprod.2c01007>

Crotofolane Diterpenoids and Other Constituents Isolated from *Croton kilwae*

Emanuel T. Mahambo, Colores Uwamariya, Masum Miah, Leandro da Costa Clementino, Luis Carlos Salazar Alvarez, Gabriela Paula Di Santo Meztler, Edward Trybala, Joanna Said, Lianne H. E. Wieske, Jas S. Ward, Kari Rissanen, Joan J. E. Munissi, Fabio T. M. Costa, Per Sunnerhagen, Tomas Bergström, Stephen S. Nyandoro,* and Mate Erdelyi*

Cite This: <https://doi.org/10.1021/acs.jnatprod.2c01007>

Read Online

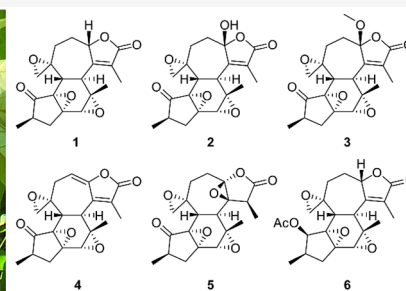
ACCESS |

Metrics & More

Article Recommendations

Supporting Information

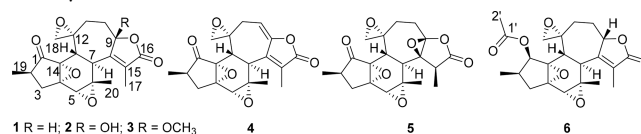
ABSTRACT: Six new crotofolane diterpenoids (1–6) and 13 known compounds (7–19) were isolated from the MeOH–CH₂Cl₂ (1:1, v/v) extracts of the leaves and stem bark of *Croton kilwae*. The structures of the new compounds were elucidated by extensive analysis of spectroscopic and mass spectrometric data. The structure of crotofilwaepoxide A (1) was confirmed by single-crystal X-ray diffraction, allowing for the determination of its absolute configuration. The crude extracts and the isolated compounds were investigated for antiviral activity against respiratory syncytial virus (RSV) and human rhinovirus type-2 (HRV-2) in HEp-2 and HeLa cells, respectively, for antibacterial activity against the Gram-positive *Bacillus subtilis* and the Gram-negative *Escherichia coli*, and for antimalarial activity against the *Plasmodium falciparum* Dd2 strain. *ent*-3 β ,19-Dihydroxykaur-16-ene (7) and ayanin (16) displayed anti-RSV activities with IC₅₀ values of 10.2 and 6.1 μ M, respectively, while exhibiting only modest cytotoxic effects on HEp-2 cells that resulted in selectivity indices of 4.9 and 16.4. Compounds 2 and 5 exhibited modest anti-HRV-2 activity (IC₅₀ of 44.6 μ M for both compounds), while compound 16 inhibited HRV-2 with an IC₅₀ value of 1.8 μ M. Compounds 1–3 showed promising antiplasmodial activities (80–100% inhibition) at a 50 μ M concentration.



The genus *Croton* (Euphorbiaceae) comprises approximately 1300 species occurring in the tropical and subtropical regions of the world,¹ of which 17 can be found in Tanzania.^{2,5} *Croton* species are used widely in folk medicine in Tanzania to treat worm infections, colds, stomachache, constipation, malaria, tuberculosis, ear infections, and cancer.⁴ The phytochemical investigations of various members of the genus *Croton* have revealed terpenoids,⁵ alkaloids,⁶ flavonoids,⁷ and diterpenoids.^{4–15} The diterpenoids include clerodanes,⁴ kauranes,¹² crotofolanes,^{8–11} labdanes,¹³ cembranes,¹⁴ and abietanes,¹⁵ some of which have exhibited cytotoxic,¹⁶ anti-inflammatory,¹² antifungal,¹⁷ acetylcholinesterase inhibition,¹⁸ and neurite outgrowth-promoting properties.¹⁹

Croton kilwae Radcl.-Sm. is a plant species endemic to Tanzania and Mozambique. In Tanzania, it grows in the Kilwa District of the Lindi Region.²⁰ The leaf morphology of *C. kilwae* resembles *C. dichogamus* Pax and *C. menyhartii* Pax.²⁰ Chemical analysis of the leaf constituents of *C. dichogamus* led to the isolation of several crotofolanes, a rare class of diterpenoids that so far have been reported from a few *Croton* species.^{8,9,11,21,22} The genus *Croton* has previously yielded interesting secondary metabolites, which makes *C. kilwae* a

suitable addition to our ongoing phytochemical investigation of *Croton* species native to Tanzania. Herein we report the isolation and structure determination of six new crotofolane diterpenoids (1–6) along with 13 known compounds (7–19) and evaluation of their antiviral, antibacterial, antiplasmodial, and cytotoxic activities.



RESULTS AND DISCUSSION

The MeOH–CH₂Cl₂ (1:1 v/v) extracts of the leaves and stem bark of *C. kilwae* were separately subjected to repeated silica

Received: November 7, 2022

gel 60 (230–400 mesh) column chromatography, followed by gel filtration on a Sephadex LH-20 column and/or HPLC. The stem bark extract yielded one new crotofolane (**1**) and six known compounds (**7**–**12**), while the leaf extract afforded six new crotofolanes (**1**–**6**) and seven known compounds (**13**–**19**, Figure S1, Supporting Information). The structures were characterized by the analysis of their spectroscopic data, including the single-crystal X-ray diffraction analysis of compound **1**. The known compounds *ent*-3 β ,19-dihydroxykaur-16-ene (**7**),^{23,24} *ent*-3 β -hydroxykaur-16-en-19-oic acid (**8**),²⁵ *ent*-16 β ,17-dihydroxykauran-19-oic acid (**9**),²⁵ *ent*-3 β ,16 α ,17-trihydroxykaurane (**10**),²⁶ 16 β ,17-dihydroxykaurane (**11**),²⁷ *ent*-3 β -hydroxykaur-16-ene (**12**),²⁸ quercetin-3-rhamnose-4,7-dimethyl ether (**13**),²⁹ 3,7,4'-tri-*O*-methylkaempferol (**14**),³⁰ 3,7,3',4'-tetra-*O*-methyl quercetin (**15**),³¹ ayanin (**16**),³² stigmasterol (**17**),³³ the pinane-type monoterpenoids 2-hydroxy-2-(hydroxymethyl)-6,6-dimethylbicyclo[3.1.1]heptan-3-one (**18**),³⁴ and *p*-hydroxyphenylethyl ferute (**19**)³⁵ were identified by comparison of their spectroscopic data (Figures S49–S145, Supporting Information) to those reported in the literature.

Compound **1**, [α]_D²⁴ –6 (*c* 0.1, CHCl₃), was obtained from both the stem bark and the leaf extracts as a white solid. Its molecular formula was established as C₂₀H₂₃O₆ based on the HRESIMS ([*M* + *H*]⁺ at *m/z* 359.1483, calcd 359.1495; Figure S9, Supporting Information) and NMR data (Table 1). The IR spectrum showed absorption bands at 1737 cm^{–1} (lactone carbonyl) and at 1666 cm^{–1} (C=C bond stretch). The ¹H NMR spectrum (Figure S2, Supporting Information) displayed a characteristic signal for an oxo-allylic proton at δ_{H} 4.92 (H-9) of a crotofolane⁸ and for the presence of three sets of methyl groups at δ_{H} 1.08 (H-20), 1.11 (H-19), and 1.97 (H-17) (Table 1). The ¹³C NMR spectrum (Figure S3, Supporting Information) displayed 20 carbons, of which two were assigned to carbonyl groups of a ketone (δ_{C} 211.0, C-1) and lactone (δ_{C} 173.3, C-16), two nonprotonated olefinic carbons [δ_{C} 161.0 (C-8), 128.4 (C-15)], and four oxygenated quaternary carbons [δ_{C} 64.2 (C-14), 61.4 (C-4), 58.4 (C-12), and 56.7 (C-6)]. The combination of ¹³C NMR and HSQC (Figures S3 and S5, Supporting Information) experiments further revealed the presence of an oxo-allylic carbon resonating at δ_{C} 82.0 (C-9), four methylene carbons at δ_{C} 57.6 (C-18), 34.1 (C-11), 32.5 (C-10), and 34.2 (C-3), three tertiary carbons at δ_{C} 36.9 (C-2), 38.0 (C-7), and 36.8 (C-13), and one epoxy carbon with a single proton at δ_{C} 57.4 (C-5).

The HMBC cross peaks (Figure 1a and Figure S6, Supporting Information) of H-17 (δ_{H} 1.97) to C-15 (δ_{C} 128.4), C-8 (δ_{C} 161.0), and C-16 (δ_{C} 173.3) indicated the presence of a methyl butenolide moiety constituting an α,β -unsaturated γ -lactone unit. The COSY and TOCSY spectra (Figures S4 and S7, Supporting Information) showed correlations between H-9 (δ_{H} 4.92) and H-17 (δ_{H} 1.97), with scalar *J* < 1 Hz as expected for long-range coupling, between H-9 and H-10 (δ_{H} 1.54, 2.47), and between H-10 (δ_{H} 1.54, 2.47) and H-11 (δ_{H} 1.61, 2.17), H-7 (δ_{H} 3.13), and H-13 (δ_{H} 2.60). This, combined with the HMBC cross peaks of H-10 (δ_{H} 1.54, 2.47) and H-11 (δ_{H} 1.61, 2.17) to C-9 (δ_{C} 82.0) and C-12 (δ_{C} 58.4) as well as H-11 (δ_{H} 1.61, 2.17) to C-13 (δ_{C} 36.8), and of H-7 (δ_{H} 3.13) to C-9 (δ_{C} 82.0), C-15 (δ_{C} 128.4), and C-8 (δ_{C} 161.0) established the seven-membered ring as being fused via C-8–C-9 of the α,β -unsaturated γ -lactone moiety.

Table 1. NMR Spectroscopic Data (500 MHz, CDCl₃) of Crotofilwaepoxide A (**1**)

position	δ_{C} , type	δ_{H} (<i>J</i> in Hz)	HMBC ^a
1	211.0, C		
2	36.9, CH	2.58 ddq (8.5, 8.4, 7.1)	C-1, C-3, C-19
3	34.2, CH ₂	1.68 dd (14.0, 8.5)	C-2, C-4, C-5, C-19
		2.92 dd (14.0, 8.4)	C-1, C-2, C-4, C-14
4	61.4, C		
5	57.4, CH	3.10 s	C-3, C-4, C-6, C-14, C-20
6	56.7, C		
7	38.0, CH	3.13 d (13.2)	C-6, C-8, C-9, C-12, C-13, C-14, C-15, C-16, C-20
8	161.0, C		
9	82.0, CH	4.92 dd (11.0, 3.7)	C-8, C-10, C-15, C-16
10	32.5, CH ₂	1.54 dddd (13.6, 12.7, 11.0, 4.4)	C-8, C-9, C-11, C-12, C-18
		2.47 dddd (12.7, 4.4, 3.7, 3.7)	C-8, C-9, C-11, C-12
11	34.1, CH ₂	1.61 ddd (13.8, 4.8, 3.7)	C-9, C-10, C-12, C-13, C-14
		2.17 ddd (13.8, 13.6, 4.4)	C-9, C-10, C-12, C-13
12	58.4, C		
13	36.8, CH	2.60 d (13.2)	C-6, C-7, C-8, C-11, C-12, C-14
14	64.2, C		
15	128.4, C		
16	173.3, C		
17	10.0, CH ₃	1.97 s	C-6, C-7, C-8, C-9, C-10, C-15, C-16
18	57.4, CH ₂	2.79 m	C-11, C-12, C-13
19	13.0, CH ₃	1.11 d (7.1)	C-1, C-2, C-3
20	20.0, CH ₃	1.08 s	C-4, C-5, C-6, C-7, C-8, C-15

^aHMBC correlations, optimized for 6 Hz, are from the stated proton(s) to the indicated carbon.

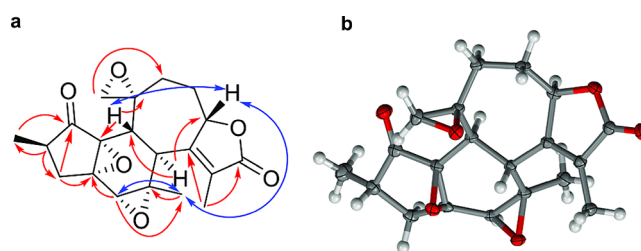


Figure 1. (a) Key HMBC (red) and NOESY (blue) correlations and (b) the X-ray crystal structure of crotofilwaepoxide A (**1**) (thermal ellipsoids at 50% probability, H₂O solvate omitted for clarity).

Furthermore, the HMBC cross peaks of H-18 (δ_{H} 2.79) to C-11 (δ_{C} 34.1), C-12 (δ_{C} 58.4), and C-13 (δ_{C} 36.8) and those of H-11 (δ_{H} 1.61, 2.17) to C-12 (δ_{C} 58.4) and C-18 (δ_{C} 57.6) indicated an epoxide group fused to the seven-membered ring. The HMBC cross peaks of H-13 (δ_{H} 2.60) to C-14 (δ_{C} 64.2) and of H-7 (δ_{H} 3.13) to C-6 (δ_{C} 56.7), as well as H-20 (δ_{H} 1.08) to C-6 (δ_{C} 56.7) and C-5 (δ_{C} 57.4), in combination with those of H-5 (δ_{H} 3.10) to C-4 (δ_{C} 61.4) and C-6 (δ_{C} 56.7) confirmed the fused six-membered ring via C-7–C-13, with the deshielded nonprotonated carbons C-4 (δ_{C} 61.4), C-12 (δ_{C}

58.4), C-6 (δ_C 56.7), and C-14 (δ_C 62.4) assigned to the corresponding epoxide carbons. Further analysis of the HMBC spectrum revealed correlations between H-19 (δ_H 1.11) and C-1 (δ_C 211.0), C-2 (δ_C 36.9), and C-3 (δ_C 34.2), and those between H-2 (δ_H 2.58) and C-1 (δ_C 211.0) and C-14 (δ_C 62.4) combined with H-3 (δ_H 2.92) and C-1 (δ_C 211.0), C-4 (δ_C 61.4), and C-14 (δ_C 62.4) suggested the presence of a cyclopentanone unit fused to a six-membered ring via C-4–C-14. The COSY and TOCSY spectra confirmed the cyclopentanone moiety through the observed correlations involving H-19 (δ_H 1.11), H-2 (δ_H 2.58), and H-3 (δ_H 1.68, 2.92).

The relative configuration in compound **1** was established based on scalar coupling constants (Table 1) and NOESY correlations (Figure S8, Supporting Information). NOEs between the methyl protons H-20 (δ_H 1.08) and H-5 (δ_H 3.10) and H-9 (δ_H 4.92), as well as between H-9 (δ_H 4.92) and H-13 (δ_H 2.60), indicated these protons to be *syn*-oriented. This was consistent with the *trans*-disposed bridgehead protons H-7 (δ_H 3.13) and H-13 (δ_H 2.60), both with $^3J_{HH} = 13.2$ Hz. To determine the absolute configuration and structure of this compound, single-crystal X-ray crystallographic analysis was performed (Figure 1b).^{36,37} The absolute configuration of **1** was determined by refinement of the Flack parameter,^{36,37} which gave the unambiguous value of 0.09(5). The configuration established for this compound is similar to previously reported crotofolanes.¹¹ Based on the spectroscopic data, this new compound (**1**) was identified as a crotofolane diterpenoid bearing C-4–C-14, C-5–C-6, and C-12–C-18 epoxide structural motifs and was given the trivial name crotofolane A (**1**).

Compound **2**, $[\alpha]_D^{24} -8$ (c 0.1, CHCl_3), was isolated from the leaf extract as a white solid. Its molecular formula, $\text{C}_{20}\text{H}_{23}\text{O}_7$, was based on the HRESIMS ($[\text{M} + \text{H}]^+ m/z$ 375.1429, calcd 375.1444 and $[\text{M} - \text{H}_2\text{O}]^+ m/z$ 357.1323; Figure S17, Supporting Information) and NMR data (Table 2). The IR spectrum showed sharp absorption bands indicative of carbonyl bond stretches of a ketone and γ -lactone at 1728 and 1761 cm^{-1} , respectively, and an intense absorption band for a hydroxy group at 3445 cm^{-1} . Comparison of NMR spectra (Figures S10–S16, Supporting Information) of **2** with those of **1** revealed their structural similarity. The absence of an oxo-allylic proton H-9 (δ_H 4.92), in combination with the large chemical shift change for C-9, which resonated at δ_C 107.8 in **2** instead of δ_C 82.0 as observed for compound **1**, suggested the presence of a hydroxy group at position C-9, forming a ketal carbon. This was confirmed by the HMBC cross peaks of proton H-7 (δ_H 3.04), H-11 (δ_H 2.38, 1.51), H-10 (δ_H 2.38, 1.93), and OH-9 (δ_H 4.32) to C-9 (δ_C 107.8) (Figure 2 and Figure S14, Supporting Information). The relative configurations of the stereocenters of compound **2** were found to be the same as those of compound **1**, based on the similar NOE correlations of protons H-5 (δ_H 3.12), H-13 (δ_H 3.16), and OH-9 (δ_H 4.32) to H-20.

Compound **3**, $[\alpha]_D^{24} +60$ (c 0.1, CHCl_3), was obtained as a white solid from the leaf extract. The HRESIMS displayed a $[\text{M} + \text{H}]^+$ peak at m/z 389.1584 (calcd 389.1600, Figure S25, Supporting Information), corresponding to a molecular formula of $\text{C}_{21}\text{H}_{24}\text{O}_7$. The IR spectrum showed a band characteristic for a carbonyl functionality at 1762 cm^{-1} . The NMR spectra (Figures S18–S24, Supporting Information) and the extracted data (Table 3) of **3** were similar to those of compounds **1** and **2**. In contrast to **1** and **2**, **3** exhibited a methoxy group at position C-9 (δ_C 109.8), instead of a proton

Table 2. NMR Spectroscopic Data (500 MHz, CDCl_3) of 9-Hydroxycrotofolane A (**2**)

position	δ_C , type	δ_H (J in Hz)	HMBC ^a
1	211.4, C		
2	36.9, CH	2.56 ddq (8.7, 8.4, 7.1)	C-1, C-3, C-4, C-19
3	34.1, CH_2	1.71 dd (13.9, 8.7) 2.90 dd (13.9, 8.4)	C-2, C-4, C-5, C-19 C-1, C-2, C-4, C-5, C-14
4	61.5, C		
5	57.7, CH	3.12 s	C-4, C-20
6	57.2, C		
7	38.0, CH	3.04 dd (12.7, 1.1)	C-6, C-8, C-9, C-13, C-15
8	158.5, C		
9	107.8, C		
OH-9		4.32 s	
10	36.7, CH_2	1.93 ddd (14.0, 13.0, 7.4) 2.38 ^b m	C-9, C-11, C-12 C-8, C-9, C-11, C-12
11	32.9, CH_2	1.51 m 2.38 ^b m	C-8, C-9, C-10, C-12, C-13, C-14, C-19 C-8, C-9, C-10, C-12
12	58.6, C		
13	35.7, CH	3.16 d (12.8)	C-6, C-7, C-8, C-11, C-12, C-14
14	64.3, C		
15	130.3, C		
16	171.1, C		
17	9.9, CH_3	1.95 d (1.1)	C-6, C-7, C-8, C-10, C-15, C-16
18	57.8, CH_2	2.79, s	C-11, C-12, C-13
19	13.1, CH_3	1.11 d (7.1)	C-1, C-2, C-3
20	20.4, CH_3	1.18 s	C-5, C-6, C-7, C-15

^aHMBC correlations, optimized for 6 Hz, are from the stated proton(s) to the indicated carbon. ^bProtons with overlapping resonances

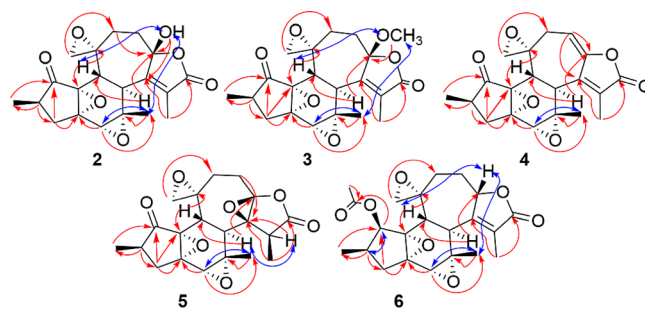


Figure 2. Key HMBC (red) and NOESY (blue) correlations of **2**–**6**.

or a hydroxy group. The position of OCH_3 -9 (δ_H 3.55, δ_C 52.0) was confirmed by the HMBC cross peak of OCH_3 -9 (δ_H 3.55) to the ketal carbon C-9 (δ_C 109.8) (Figure 2 and Figure S22, Supporting Information). Therefore, compound **3** was identified as the new crotofolane 9-methoxycrotofolane A (**3**), being an *O*-methylated derivative of compound **2**.

Compound **4**, $[\alpha]_D^{24} +36$ (c 0.07, CHCl_3), was isolated from the leaf extract as a white solid. Its molecular formula, $\text{C}_{20}\text{H}_{21}\text{O}_6$, was based on the HRESIMS ($[\text{M} + \text{H}]^+ m/z$ 357.1324, calcd 357.1338; Figure S33, Supporting Information) and NMR data (Table 4). The IR spectrum showed bands at 1660 and 1738 cm^{-1} , which are indicative for ketone

Table 3. NMR Spectroscopic Data (500 MHz, CDCl₃) of 9-Methoxycrotokilwaepoxide A (3)

position	δ_C , type	δ_H (J in Hz)	HMBC ^a
1	211.3, C		
2	36.9, CH	2.57, ddq (8.4, 8.4, 7.1)	C-1, C-3, C-19
3	34.2, CH ₂	1.69 dd (13.9, 8.4) 2.90 dd (13.9, 8.4)	C-2, C-4, C-5, C-19
4	61.4, C		
5	57.8, CH	3.09 s	C-3, C-4, C-6, C-20
6	57.3, C		
7	38.0, CH	3.02 d (12.8)	C-6, C-8, C-9, C-13, C-14, C-15
8	158.7, C		
9	109.8, C		
OMe-9	52.0, CH ₃	3.55 s	C-9
10	30.5, CH ₂	1.75 ddd (15.0, 13.9, 4.0) 2.67 ddd (15.0, 3.9, 3.6)	C-9, C-11, C-12 C-8, C-9, C-11, C-12
11	32.9, CH ₂	1.49 ddd (13.8, 4.0, 3.6) 2.15 ddd (13.9, 13.8, 3.9)	C-9, C-10, C-13, C-18 C-9, C-10, C-12, C-13
12	58.4, C		
13	35.7, CH	3.07 d (12.8)	C-7, C-8, C-11, C-12, C-14, C-18
14	64.3, C		
15	129.9, C		
16	170.8, C		
17	10.0, CH ₃	1.95 s	C-6, C-7, C-8, C-9, C-10, C-15, C-16
18	57.9, CH ₂	2.78 s	C-11, C-12, C-13
19	13.1, CH ₃	1.11 d (7.1)	C-1, C-2, C-3
20	20.5, CH ₃	1.15 s	C-6, C-7

^aHMBC correlations, optimized for 6 Hz, are from the stated proton(s) to the indicated carbon.

Table 4. NMR Spectroscopic Data (500 MHz, CDCl₃) of Crotokilwaepoxide B (4)

position	δ_C , type	δ_H (J in Hz)	HMBC ^a
1	210.9, C		
2	37.1, CH	2.59 ddq (8.5, 8.4, 7.1)	C-1, C-3, C-19
3	34.2, CH ₂	1.71 dd (13.9, 8.5) 2.93 dd (13.9, 8.4)	C-2, C-4, C-5, C-19 C-1, C-2, C-4, C-14
4	61.4, C		
5	58.0, CH	3.10 s	C-3, C-4, C-6, C-14, C-20
6	57.3, C		
7	38.7, CH	3.14 dq (12.7, 1.6)	C-6, C-8, C-9, C-13, C-14, C-15, C-16, C-20
8	147.2, C		
9	149.3, C		
10	109.4, CH	5.81 ddd (6.9, 2.9, 0.9)	C-8, C-9, C-11, C-12, C-14
11	38.0, CH ₂	2.17 dd (16.9, 6.9) 3.21 ddd (16.9, 2.9, 1.0)	C-8, C-9, C-10, C-12, C-13, C-14, C-15, C-18 C-9, C-10, C-12
12	57.1, C		
13	36.6, CH	2.79 dd (12.7, 1.0)	C-4, C-7, C-8, C-12, C-14
14	64.6, C		
15	130.7, C		
16	169.4, C		
17	11.1, CH ₃	2.09 dd (1.6, 0.9)	C-6, C-7, C-8, C-9, C-10, C-15, C-16
18	56.5, CH ₂	2.83 d (3.9) 2.87 d (3.9)	C-10, C-11, C-12 C-4, C-11, C-12, C-14
19	13.0, CH ₃	1.13 d (7.1)	C-1, C-2, C-3
20	19.6, CH ₃	1.12 s	C-5, C-6, C-7, C-8, C-13, C-15

^aHMBC correlations, optimized for 6 Hz, are from the stated proton(s) to the indicated carbon.

and γ -lactone moieties, respectively. The NMR spectra (Figures S26–S32) of **4** suggested it to have a similar carbon structural scaffold to compounds **1–3**. However, the spectra for compound **4** differed from those of **1–3** for signals associated with C-9 (δ_C 149.3) and C-10 (δ_C 109.4, δ_H 5.81), indicative of an endocyclic double bond between C-9 and C-10, presumably formed via enzymatically mediated dehydration of compound **2**. The positions of the carbons generating these signals were confirmed by the HMBC (Figure 2 and Figure S30, Supporting Information) cross peaks of H-11 (δ_H 2.17, 3.21), H-7 (δ_H 3.14), and H-10 (δ_H 5.81) to C-9 (δ_C 149.3) and those of H-11 (δ_H 2.17, 3.21) and H-18 (2.83, 2.87) to C-10 (δ_C 109.4). Moreover, coupling between the olefinic proton H-10 (δ_H 5.81) and the diastereotopic protons H-11 (δ_H 3.21, 2.17) was observed in the COSY spectrum (Figure S28, Supporting Information). The relative configurations of **4** were determined to be the same as those of compounds **1–3** for the stereogenic centers these compounds have in common (Figure 2 and Figure S32, Supporting Information). Thus, this new compound, crotokilwaepoxide B (**4**), was characterized as the C-9–C-10 dehydrated derivative of compound **2**.

Compound **5**, [α]_D²⁴ –29 (c 0.1, CHCl₃), was isolated from the leaf extract as a white solid. Its molecular formula, C₂₀H₂₃O₇, was determined from the HRESIMS (m/z 375.1432 [M + H]⁺, calcd 375.1444; Figure S41, Supporting Information) and NMR data (Table 5). The IR spectrum

revealed absorption bands at 1741 and 1799 cm⁻¹, which could be attributed to a ketone and lactone functionality, respectively. Analysis of the NMR spectra (Figures S34–S40, Supporting Information) of **5** revealed it to have a crotolane skeleton similar to compounds **1–4**. However, contrary to the NMR spectroscopic data for **1–3** that indicated an α,β unsaturated γ -lactone moiety in each case, the ¹³C NMR spectrum (Figure S35, Supporting Information) of **5** suggested the saturation of C-15 (δ_C 45.5) and C-8 (δ_C 65.8). In addition, the COSY spectrum (Figure S36, Supporting Information) indicated an isolated coupling between the CH₃-17 methyl protons (δ_H 1.48, d, J = 7.5 Hz) and the H-15 proton (δ_H 3.14, q, J = 7.5 Hz). The chemical shift of C-8 (δ_C 65.8) and that of C-9 (δ_C 89.9) were consistent with epoxidation at C-8 and C-9, which was confirmed by the HMBC cross-peaks (Figure 2 and Figure S38, Supporting Information) of protons H-15 (δ_H 3.14), H-10 (δ_H 2.18, 2.78), H-17 (δ_H 1.48), and H-7 (δ_H 2.44) to C-8 (δ_C 65.8) as well as H-10 (δ_H 2.18, 2.78) and H-11 (δ_H 2.64) to C-9 (δ_C 89.9). The relative configuration of C-8 and C-9 could not be determined from the NMR data obtained. However, the relative configuration at C-15 for **5** was established through the NOE interaction of H-15 (δ_H 3.14) with H-7 (δ_H 2.44). The other configurations of the stereogenic centers of **5** were established to be identical to **1**, based on similar NOE correlations for the two compounds observed (Figure 2 and

Table 5. NMR Spectroscopic Data (500 MHz, CDCl₃) of Crotokilwaepoxide C (5)

position	δ_C , type	δ_H (J in Hz)	HMBC ^a
1	210.8, C		
2	37.0, CH	2.54 ddq (8.4, 8.3, 7.2)	C-1, C-3, C-19
3	34.2, CH ₂	1.68 dd (14.0, 8.4) 2.90 dd (14.0, 8.3)	C-2, C-4, C-5, C-19 C-1, C-2, C-4, C-14
4	61.6, C		
5	58.0, CH	3.02 s	C-3, C-4, C-6, C-14, C-20
6	56.9, C		
7	39.8, CH	2.44 d (13.0)	C-5, C-6, C-8, C-13, C-14, C-15, C-20
8	65.8, C		
9	89.9, C		
10	24.7, CH ₂	2.18 ddd (15.7, 12.9, 7.7) 2.78 ddd (15.7, 6.2, 1.3)	C-9, C-11 C-8, C-9, C-11, C-12
11	33.6, CH ₂	1.61 ddd (15.1, 12.9, 6.2) 2.64 ddd (15.1, 7.7, 1.3)	C-10, C-12, C-13 C-9, C-10, C-12, C-18
12	58.6, C		
13	32.8, CH	2.54 d (13.0)	C-6, C-7, C-8, C-11, C-12, C-14
14	64.1, C		
15	45.5, CH	3.14 q (7.5)	C-7, C-8, C-16, C-17
16	175.7, C		
17	10.5, CH ₃	1.48 d (7.5)	C-8, C-15, C-16
18	52.4, CH ₂	2.72 d (4.0) 2.78 d (4.0)	C-7, C-11, C-12 C-10, C-13
19	13.2, CH ₃	1.10 d (7.2)	C-1, C-2, C-3
20	21.6, CH ₃	1.48 s	C-5, C-6, C-7

^aHMBC correlations, optimized for 6 Hz, are from the stated proton(s) to the indicated carbon.

Figure S40, Supporting Information). This new compound, crotokilwaepoxide C (5), was therefore characterized as the C-8–C-9 epoxy derivative of 1.

Compound 6, [α]_D²⁴ –20 (c 0.05, CHCl₃), was obtained from the leaf extract as a colorless oil with the molecular formula C₂₂H₂₇O₇, as established by HRESIMS ([M + H]⁺ at *m/z* 403.1744, calcd 403.1757; Figure S49, Supporting Information) and NMR data (Table 6). The IR spectrum showed a band at 1744 cm⁻¹, which was indicative of a carbonyl group. The NMR spectra (Figures S42–S48, Supporting Information) of 6 resembled those of 1 except for the presence of an additional oxymethine proton signal at δ_H 5.53 and that of a deshielded methyl group at δ_H 2.19, which were assigned to H-1 and H-2', respectively, with their corresponding carbons at δ_C 75.6 and 20.9. The ¹³C NMR spectrum (Figure S43, Supporting Information) showed one more additional signal at δ_C 170.0 (C-1'), with HMBC to H-1 (δ_H 5.53) and H-2' (δ_H 2.19) (Figure 2 and Figure S46, Supporting Information), indicating the formation of an acetate moiety at C-1 instead the carbonyl group as present for compounds 1–5. The position of the acetate group was confirmed by the HMBC cross peaks of proton H-3 (δ_H 2.45) and H-19 (δ_H 0.95) to C-1 (δ_C 75.6). The relative configuration at C-1 for 6 was based on the NOE correlation between H-1 (δ_H 5.53) and H-2 (δ_H 2.15) (Figure 2 and Figure S48, Supporting Information), along with their scalar coupling constant (³J_{HH} = 5.4 Hz) that indicated a *syn* orientation. The other configurations at the stereogenic centers

Table 6. NMR Spectroscopic Data (500 MHz, CDCl₃) of Crotokilwaepoxide D (6)

position	δ_C , type	δ_H (J in Hz)	HMBC ^a
1	75.6, CH	5.53 d (5.3)	C-3, C-4, C-14, C-1'
2	33.1, CH	2.15 ^b dddd (10.3, 7.2, 7.0, 5.3)	
3	36.4, CH ₂	1.63 dd (13.8, 10.3) 2.45 ^b (13.8, 7.2)	C-2, C-4, C-19 C-1, C-4, C-14
4	61.0, C		
5	57.4, CH	3.10 s	C-4, C-6, C-14, C-20
6	55.9, C		
7	38.1, CH	3.12 dd (12.9, 1.3)	C-6, C-8, C-9, C-13, C-15, C-20
8	161.7, C		
9	81.9, CH	4.92 m	
10	32.5, CH ₂	1.51 ^b m 2.42 ^b m 1.50 ^b m	C-7, C-9, C-11, C-12, C-13, C-18 C-8, C-9, C-11, C-12 C-7, C-9, C-10, C-12, C-13, C-18
11	34.6, CH ₂	1.75 ddd (15.0, 15.0, 4.4)	C-9, C-10, C-13
12	58.7, C		
13	37.4, CH	2.38 d (12.9)	C-6, C-7, C-8, C-11, C-12, C-14, C-18
14	66.8, C		
15	128.2, C		
16	173.4, C		
17	10.0, CH ₃	1.96 dd (1.4, 1.4)	C6, C-8, C-9, C-10, C-15, C-16
18	57.0, CH ₂	2.86 d (4.7) 3.18, d (4.7)	C-11, C-12 C-10, C-11, C-12
19	12.4, CH ₃	0.95, d (7.0)	C-1, C-2, C-3
20	20.2, CH ₃	1.09, s	C-5, C-6, C-7
1'	170.0, C		
2'	20.9, CH ₃	2.19 ^b s	C-1, C-1'

^aHMBC correlations, optimized for 6 Hz, are from the stated proton(s) to the indicated carbon. ^bOverlapping signals.

of 6 were similar to those of 1 and of another related compound previously confirmed by X-ray crystallographic analysis.²¹ Therefore, the new compound crotokilwaepoxide D (6) was characterized as the C-1 acetoxy derivative of 1. Crotofolanes 1–6 are similar to the crotoascarins published by Kawakami et al.²² and have identical configurations. However, their side chains are different, and they have an epoxide at C-12–C-18 instead of an alkene.

Crotofolanes are rare diterpenoids that have been previously reported from several *Croton* species including *C. corylifolios*,^{24,38} *C. dichogamus*,^{9,39} *C. haumanianus*,²¹ *C. cascarilloides*,^{10,11,22} *C. caracasanus*,⁸ and *C. megalocarpus*.⁴⁰ This unusual skeleton has been hypothesized to be biosynthesized from geranyl pyrophosphate, which is subsequently transformed via cembrane, casbane, and lathyrane to crotofolanes.¹⁰ Compounds 1–6 presented in this study are multiepoxidized crotofolanes having the unprecedented epoxidation of the exocyclic double bond found on the heptacyclic ring of the previously reported analogues, with compound 5 having an additional epoxide moiety. All ¹³C NMR chemical shifts for compounds 1–6 were in good agreement with those predicted by CSearch.⁴¹ *C. kilwae* was recently reported to be in the same clade as *C. dichogamus*,⁴² one of the *Croton* species reported to biosynthesize crotofolanes.^{3,9,39} Therefore, the present findings provide additional insight into the chemotaxonomic relation-

ships among *Croton* species, which warrant further investigations.

The crude extracts and the isolated compounds from *C. kilwae* were tested for antiviral activity against both HRV-2 and RSV. The antiviral activities against RSV are given in Table S1, and the dose response for the most active compounds (7 and 16) is presented in Figure S147 (Supporting Information). Compounds 7 and 16 showed anti-RSV activity with IC_{50} values of 10.2 and 6.1 μM , while marginal cytotoxic effects (CC_{50}) on HEp-2 cells were observed, which resulted in selectivity index (SI; CC_{50}/IC_{50}) values of 4.9 and 16.4, respectively. Lopes et al. reported⁴³ that acetylation of quercetin enhanced the virucidal activity of this compound against RSV particles. Since compound 16 is a 3,7,4'-tri-*O*-methylated derivative of quercetin, it was investigated for the occurrence of this type of activity. However, it exhibited no RSV particle inactivating (virucidal) activity at the doses tested. The anti-HRV-2 activity of selected compounds is shown in Table S2 (Supporting Information). Compounds 2 and 5 inhibited HRV-2 at relatively high concentrations only (IC_{50} of 44.6 μM for both, SI > 2.2). However, compound 16, besides its anti-RSV activity, also exhibited anti-HRV-2 activity with an IC_{50} value of 1.8 μM . Using the MTS (tetrazolium)-based cytotoxicity assay no substantial toxicity of 16 for HeLa cells was observed at a concentration of $\leq 100 \mu\text{M}$ (SI > 55.6); however, microscopic observation revealed the presence of morphological alterations in HeLa cells treated with 16 at $\geq 20 \mu\text{M}$ (Table S2, Supporting Information). Compound 16 is also known for its antimicrobial activity against *Mycobacterium tuberculosis*.⁴⁴ Crotofilanes 1–5 gave IC_{50} and CC_{50} values of >100 μM , which indicated a lack of both anti-RSV activity and cytotoxicity for HEp-2 cells at concentrations up to 100 μM (Table S1, Supporting Information). Indeed, similar compounds have been shown to be nontoxic to the PC-3, HeLa, and MCF-7 human tumor cell lines, exhibiting CC_{50} values of >50 μM .⁸ In our hands, compounds 1, 2, 4, and 5 showed no cytotoxicity at $\leq 100 \mu\text{M}$ for HeLa and HEp-2 cells. Similar compounds have recently been reported to inhibit HIV-1 replication,^{3,40} indicating the biomedical potential of these types of natural products. Neither the crude extracts nor the isolated pure compounds showed antibacterial activities against *Bacillus subtilis* or *Escherichia coli* at a $\sim 2 \text{ mM}$ concentration.

Compounds 1–6 were tested against chloroquine-resistant⁴⁵ *Plasmodium falciparum* Dd2 cells at 50 μM (Figure 3 and Table S3, Supporting Information). The most active compounds, 1–3, inhibited parasite growth at 80–100%, whereas compounds 4, 5, and 6 controlled parasitemia at 26%, 42%, and 60%, respectively. For all compounds, low (<10%) or no hemolysis was observed (Figure S142, Supporting Information). The present results suggest that crotofilane diterpenoids may be interesting compound scaffolds for antimalarial drug development.

In conclusion, six new crotofolanes (1–6) and 13 known compounds (7–19) were isolated from *C. kilwae* leaf and stem bark extracts. Compounds 7 and 16 showed anti-RSV activity, and compounds 2, 5, and 16 inhibited HRV-2 in HeLa cells. Compounds 1–3 displayed antiplasmodial activities at a 50 μM concentration. The isolation of crotofilane diterpenoids from *C. kilwae* is of chemotaxonomic significance.

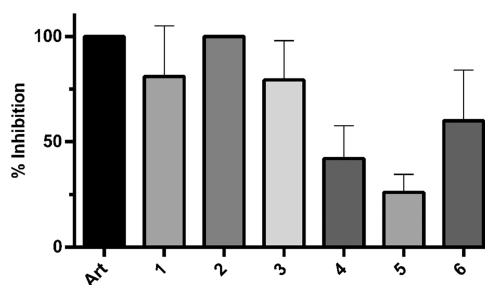


Figure 3. In vitro growth inhibition of asexual blood stage *P. falciparum* (Dd2) for crotofolanes 1–6. The inhibitory potential was tested at a concentration of 50 μM , and the inhibition of parasitemia was measured after 72 h of incubation. The data are from at least two independent experiments shown as the average \pm standard deviation (artesunate and 2 gave 100% inhibition for all replicates, and therefore no standard deviation is given). Art: artesunate, 5 μM .

EXPERIMENTAL SECTION

General Experimental Procedures. Optical rotations were measured using a 341 LC OROT polarimeter (589 nm, 24.0 °C). UV spectra were obtained in CH_2Cl_2 using a Shimadzu UV-1650PC UV/vis spectrophotometer. Infrared (IR) spectra were recorded on a PerkinElmer Spectrum FT-IR instrument using liquid/solid samples. NMR spectra were acquired on a Bruker Avance NEO 500 MHz NMR spectrometer equipped with a 5 mm TXO cryogenic probe and were processed using the MestReNova (v14.0.0) software. Chemical shifts were referenced to the residual carbon and proton signals of the deuterated solvents (CDCl_3 δ_{H} 7.26 and 77.2 or CD_3OD δ_{H} 4.87 and 49.0) as internal standards. HRESIMS spectra were obtained with a Q-TOF-LC/MS spectrometer using a 2.1 \times 30 mm 1.7 μM RPC18 and $\text{H}_2\text{O}-\text{CH}_3\text{CN}$ gradient (5:95–95:5 in 0.2% formic acid, v/v) at Stenhagen Analys Lab AB, Gothenburg, Sweden. Silica gel 60 (230–400 mesh) and Sephadex LH-20 (GE Healthcare) were used for column chromatography. Percolated silica gel plates (Merck F₂₅₄) were used for thin layer chromatography, which were visualized under UV light at 254 nm and stained with 4-anisaldehyde (7:5:8:180; volume ratio of 4-anisaldehyde, concentrated H_2SO_4 , glacial acetic acid, and MeOH), followed by gentle heating, to visualize UV-inactive compounds and characteristic color changes of UV-positive spots. Preparative reversed-phase (RP)-HPLC was performed on a VWR LaPrep P110 instrument with single-wavelength detection, 220 nm, using a chiral column, Phenomenex Lux Amylose-1 column (5 μm , 1000 Å, Φ 21.2 mm, L 250 mm), with isocratic elution using $\text{CH}_3\text{CN}-\text{H}_2\text{O}$ (3:7, v/v) as mobile phase and a flow-rate of 15 mL/min. The method was optimized on an analytical HPLC instrument (VWR LaChrome Elite system) with a Phenomenex Lux Amylose-1 column (5 μm , 1000 Å, Φ 4.6 mm, L 100 mm) and a flow-rate of 1.0 mL/min.

Plant Material. The stem bark and leaves of *C. kilwae* were collected in November 2018 along a road to Rushungi (4 km outside of the village) at GPS location S 09°27.55.1 E 039°36.17.3 at an elevation of 103 m in the Kilwa District of the Lindi Region, Tanzania. The plant was identified and authenticated by F. M. Mbago, a senior taxonomist of the herbarium at the Botany Department of the University of Dar es Salaam, where a voucher specimen (FMM 3904) was deposited.

Extraction and Isolation. The air-dried and pulverized leaves (1.8 kg) and stem bark (1.2 kg) were extracted with $\text{MeOH}-\text{CH}_2\text{Cl}_2$ (1:1) twice for 48 h at room temperature. Upon concentration of each extract using a rotary evaporator at 40 °C, 130 and 100 g of leaf and stem bark crude extracts, respectively, were obtained. The dried leaf extract (130 g) was subjected to silica gel column chromatography and eluted with a gradient system of EtOAc–*n*-hexane (10:90 to 100 EtOAc) followed by 5% MeOH in EtOAc to afford 140 fractions, which were combined into nine pooled fractions (chronologically labeled FL1–FL9) based on TLC characteristics. Compound 1 (8 mg) was isolated from FL8 after further purification by Sephadex

column chromatography LH-20 (MeOH–CH₂Cl₂, 1:1) and subsequent purification of fractions 11–24 by another silica gel column (MeOH–CH₂Cl₂, 1:4). Compounds 2 (6.4 mg) and 4 (4.3 mg) were obtained after FL6 was subjected to Sephadex column chromatography LH-20 (MeOH–CH₂Cl₂, 1:1) and further purification by gel column chromatography (EtOAc–CH₂Cl₂, 1:4). FL4 yielded compounds 3 (3.8 mg) and 18 (6 mg) after purification by Sephadex column chromatography LH-20 (MeOH–CH₂Cl₂, 1:1) and subsequent silica gel chromatography (EtOAc–CH₂Cl₂, 0.5:9.5). Compound 3 was obtained after preparative TLC (MeOH–EtOAc–*n*-hexane, 1:3:6) of subfractions 4–7 eluted from the second silica gel column. Compound 15 (25 mg) was isolated from FL2 after further purification by Sephadex LH-20 column chromatography (MeOH–CH₂Cl₂, 1:1) and the washing of subfractions 11–18 with *n*-hexane. Compound 7 (2 mg) was obtained after purification of fraction FL3 by Sephadex LH-20 column chromatography (MeOH–CH₂Cl₂, 1:1). Compounds 5 (7.2 mg) and 14 (14 mg) were isolated from FL1 after purification of subfractions 7–21, obtained from the Sephadex LH-20 column (MeOH–CH₂Cl₂, 1:1), utilizing a second silica gel column (EtOAc–CH₂Cl₂, 1:9). From the second silica gel column, compound 14 was eluted as subfractions 1 and 2, whereas compound 5 required an additional purification step of subfractions 3–6 by further silica gel column chromatographic separation (EtOAc–CH₂Cl₂, 0.5:9.5). Compounds 1 (3 mg) and 6 (2 mg) were obtained from FL7 after isolation by Sephadex LH-20 column chromatography (MeOH–CH₂Cl₂, 1:1), of which subfractions 8–19 were further purified by silica gel column chromatography (EtOAc–CH₂Cl₂, 3:7) and collection of subfractions 8–11. The final compounds were separated by RP-HPLC chromatography (CH₃CN–H₂O, 3:7) with retention times of 5.89 and 11.41 min for compounds 1 and 6, respectively. Compounds 16 (20 mg) and 19 (5.7 mg) were obtained after purification of FL5 and FL9, respectively, by Sephadex LH-20 column chromatography (MeOH–CH₂Cl₂, 1:1).

The stem bark extract (100 g) of *C. kilwae* was fractionated by silica gel column chromatography with a gradient elution of an EtOAc–petroleum ether solvent system with increasing polarity from 10% EtOAc in petroleum ether to 100% EtOAc and then 5% MeOH in EtOAc, to afford 110 fractions. Based on TLC profiling, the obtained fractions were pooled into 14 fractions labeled FSB1–FSB14. Compounds 1 (5 mg), 9 (5 mg), and 10 (4.3 mg) were all isolated from FSB12 after purification of subfractions 30–44 using a second silica gel column (EtOAc–petroleum ether, 2:3) and a third silica gel column (EtOAc–CH₂Cl₂, 1:4). Compound 1 was obtained from washing subfractions 4–9 eluted from the third silica column with MeOH. Compound 9 was obtained after subjecting subfractions 60–80 from the third silica column to passage over another silica column (EtOAc–CH₂Cl₂, 1:4) and further purification using Sephadex LH-20 (100% MeOH). Isolation of compound 10 was achieved after further purification of subfractions 45–59 from the third silica column with an additional silica gel column (EtOAc–CH₂Cl₂, 1:4). Compounds 8 (4 mg) and 13 (5 mg) were obtained from fraction FSB11 after purification by silica gel column chromatography (EtOAc–petroleum ether, 2:3). Subfractions 57–66 were further purified by silica gel column chromatography (EtOAc–CH₂Cl₂, 1:4) and subsequent Sephadex LH-20 column chromatography (100% MeOH) to yield compound 8. Subfractions 26–36 from the first silica gel column performed on FSB11 were subjected to Sephadex LH-20 column chromatography (MeOH–CH₂Cl₂, 1:1) followed by a final column chromatographic step on silica gel (EtOAc–CH₂Cl₂, 1:9) to afford compound 13. Compound 17 (60 mg) was isolated from fraction FSB6 after further purification by silica gel column chromatography (EtOAc–petroleum ether, 1:4). Compound 11 (10 mg) was isolated from fraction FSB10 after purification by silica gel column chromatography (EtOAc–CH₂Cl₂, 1:9), from which subfractions 42–46 were further purified by Sephadex LH-20 column chromatography (MeOH–CH₂Cl₂, 1:1) and subsequent preparative TLC (EtOAc–CH₂Cl₂, 1:9). Compound 12 (6.3 mg) was obtained from fraction FSB5 after purification by Sephadex LH-20 gel column

chromatography (MeOH–CH₂Cl₂, 1:1) and crystallization of subfractions 8–13 from MeOH.

Crotokilwaepoxide A (1): white solid; $[\alpha]_D^{24}$ –6 (*c* 0.1, CHCl₃); IR ν_{\max} 2930, 1737, 1666, 1444, 1096, 1018, 928, 905 cm⁻¹; ¹H and ¹³C NMR, see Table 1; HRESIMS *m/z* 359.1483, [M + H]⁺ (calcd *m/z* 359.1495 for C₂₀H₂₃O₆).

9-Hydroxycrotokilwaepoxide A (2): white solid; $[\alpha]_D^{24}$ –8 (*c* 0.1, CHCl₃); IR ν_{\max} 3445, 2936 1761, 1730, 1436, 1329, 954, 906 cm⁻¹; ¹H and ¹³C NMR, see Table 2; HRESIMS *m/z* 357.1323 [M – H₂O]⁺ and *m/z* 357.1323 [M + H]⁺ (calcd *m/z* 374.1366 for C₂₀H₂₃O₇).

9-Methoxycrotokilwaepoxide A (3): white solid; $[\alpha]_D^{24}$ +60 (*c* 0.1, CHCl₃); IR ν_{\max} 2932, 1762, 1445, 1318, 1123, 969, 906 cm⁻¹; ¹H and ¹³C NMR, see Table 3; HRESIMS *m/z* 389.1584 [M + H]⁺ (calcd *m/z* 389.1600 for C₂₁H₂₅O₇).

Crotokilwaepoxide B (4): white solid; $[\alpha]_D^{24}$ +36 (*c* 0.07, CHCl₃); IR ν_{\max} 2924, 1738, 1660, 1447, 1410, 1066, 907, 890 cm⁻¹; ¹H and ¹³C NMR, see Table 4; HRESIMS *m/z* 357.1324 [M + H]⁺ (calcd *m/z* 357.1338 for C₂₀H₂₁O₆).

Crotokilwaepoxide C (5): white solid; $[\alpha]_D^{24}$ –29 (*c* 0.1, CHCl₃); IR ν_{\max} 2923, 2852, 1799, 1741, 1456, 1377, 970, 890 cm⁻¹; ¹H and ¹³C NMR, see Table 5; HRESIMS *m/z* 375.1432 [M + H]⁺ (calcd *m/z* 375.1444 for C₂₀H₂₃O₇).

Crotokilwaepoxide D (6): white solid; $[\alpha]_D^{24}$ –20 (*c* 0.05, CHCl₃); IR ν_{\max} 2924, 1744, 1232, 1019, 801 cm⁻¹; ¹H and ¹³C NMR, see Table 6; HRESIMS *m/z* 403.1744 [M + H]⁺ (calcd *m/z* 403.1757 for C₂₂H₂₇O₇).^{36,37}

X-ray Diffraction Analysis. SCXRD measurements were performed using a Rigaku SuperNova dual-source Oxford diffractometer equipped with an Atlas detector using mirror-monochromated Cu K α (λ = 1.54184 Å) radiation. The data collection and reduction were performed using the program CrysAlisPro, and a Gaussian face index absorption correction method was applied.⁴⁶ The structures were solved by intrinsic phasing (SHELXT)⁴⁷ and refined by full-matrix least-squares techniques against F² using all data (SHELXL).⁴⁷ All non-hydrogen atoms were refined with anisotropic displacement parameters. Hydrogen atoms were constrained in geometric positions to their parent atoms using OLEX2.

X-ray Crystallographic Data of Compound 1. Diffraction-quality crystals were obtained from dichloromethane. Crystal data for compound 1: 2(C₂₀H₂₂O₆)·H₂O, M = 734.77, colorless block, 0.18 × 0.31 × 0.46 mm, monoclinic, space group I2 (no. 5), *a* = 14.5703(2) Å, *b* = 8.6823(1) Å, *c* = 14.1008(2) Å, β = 103.077(1)°, *V* = 1737.54(4) Å³, *Z* = 2, *T* = 120.0(1) K, μ = 0.87 mm⁻¹, *D*_{calc} = 1.404 g cm⁻³, *F*(000) = 780, 7982 measured reflections (7.8° ≤ 2 θ ≤ 152.6°), 3425 unique reflections (*R*_{int} = 0.017), which were used in all calculations. The final *R*₁ was 0.031 (*I*_o > 2 σ (*I*_o)) and *wR*₂ was 0.084 (all data). The Flack parameter^{36,37} was 0.09(5). The X-ray structure of 1 (CCDC-2209300) has been deposited at the Cambridge Crystallographic Data Centre.⁴⁸ Copies of the data can be obtained, free of charge, on application to the Director, CCDC, 12 Union Road, Cambridge CB2 1EZ, UK (fax: + 44-(0)1223-336033 or email: deposit@ccdc.cam.ac.uk).

Antiviral Assays. Human laryngeal epidermoid carcinoma (HEp-2) cells were used for the testing of antirespiratory syncytial virus (RSV) and the cytotoxic activities of both crude extracts and the pure compounds isolated therefrom, while the human uterine cervical cancer cells (HeLa) were employed for similar assays performed with human rhinovirus type 2 (HRV-2). The anti-RSV plaque assay was performed as described by Mollel et al.⁴⁹ Briefly, serial 5-fold dilutions of the test sample in maintenance DMEM (Dulbecco's modified Eagle's medium supplemented with 2% heat-inactivated fetal calf serum, 1% pest stock, and 1% L-glutamine stock) were added to HEp-2 cells growing in a cluster 24-well plate and incubated at 37 °C for 15 min in a humidified atmosphere comprising 5% CO₂ (the CO₂ incubator). Subsequently, 50 μ L of fresh DMEM comprising approximately 100 plaque-forming units of RSV A2 strain⁵⁰ (ATCC, VR-1540) was added and placed in the CO₂ incubator for a further 2.5 h. The final concentrations of the samples tested were

100, 20, 4, 0.8, 0.16, and 0.0 μM . Then, the virus–test sample mixture was removed, and the cells were overlaid with 1% methylcellulose solution in DMEM that comprised the same concentrations of the test sample. The assay plates were left for 3 days in the CO_2 incubator, then stained with a 0.75% solution of crystal violet, with the developed RSV plaques counted under a microscope.

The anti-HRV-2 activity of the test samples was assayed as follows. The HeLa cells growing in cluster 96-well plates received 60 μL of maintenance EMEM (Eagle's minimum essential medium supplemented with 2% fetal calf serum, 1% pest stock, 1% L-glutamine stock, 30 mM MgCl_2 , and 20 mM HEPES (pH 7.1)) and 20 μL of serial 5-fold dilutions of the test sample in EMEM. The assay plates were left in the CO_2 incubator at 34 $^\circ\text{C}$ for 3 h, and then the cells with test samples received 20 μL of fresh EMEM comprising approximately 100 tissue culture infectious doses (TCID_{50}) of HRV-2 strain HGP (ATCC, VR-482). The final concentrations of the samples tested were 100, 20, 4, 0.8, 0.16, and 0.0 μM . Following incubation in the CO_2 incubator for 3 days, the cells were stained with crystal violet to visualize any protection of cells against the virus-induced cytopathic effect.

Cytotoxicity of the crude extracts and pure compounds for HEp-2 cells was tested as described by Mollel et al.⁴⁹ Briefly, the cells, seeded in cluster 96-well plates the day prior to the experiment, were rinsed with DMEM, and 50 μL of fresh DMEM was added. Then, the cells received 50 μL of DMEM that comprised the test compounds at 5-fold increasing concentrations within a range of 0.16–100 μM or 0.16–100 $\mu\text{g}/\text{mL}$ for the crude extracts. After incubation of cells with the test samples for 3 days in the CO_2 incubator, 15 μL of the CellTiter 96 AQueous One Solution reagent (Promega, Madison, WI, USA) was added. The assay plates were shaken and left in the incubator for a further 1–2 h, and the absorbance of the samples was recorded at 490 nm. Cytotoxicity of the test samples for HeLa cells was performed in the same manner, except that EMEM was used instead of DMEM as the maintenance medium.

Antibacterial Assays. The antibacterial activity of the isolated compounds was evaluated against *Bacillus subtilis* strain YB866 (Gram-positive) and *Escherichia coli* strain MG1655 (Gram-negative). The compounds were dissolved in DMSO according to their solubility and stored at -20 $^\circ\text{C}$. Bacterial species were cultured as previously described by Mueller and Hinton⁵¹ and Doyle et al.⁵² For the determination of antibacterial activity, bacterial cells were grown overnight in cation-adjusted Mueller-Hinton II broth (MHB). The culture was diluted to $\text{OD} = 0.05$ in MHB. The concentration of the compounds tested was 3% v/v in 10 μL as the final volume (see Supporting Information). The assay was carried out in transparent 384-well plates at 37 $^\circ\text{C}$ without agitation for 18 h. After incubation, viability was measured by adding 1 μL of resazurin (AlamarBlue) per well and incubating at 37 $^\circ\text{C}$ for 1–2 h. Fluorescence was measured with a POLARstar Omega microplate reader (544–590 nm). Cells exposed to 3% v/v of DMSO were used as a positive control. The assay was performed in three independent replicates. Results are presented as the fluorescence mean normalized by the fluorescence of the positive control. The cutoff for *B. subtilis* was 0.1 and that for *E. coli* was 0.5; compounds with higher values were considered as nonactive against bacteria.

Antiplasmodial Assays. For *P. falciparum* antiplasmodial assays, the chloroquine-resistant strain (Dd2) used in this study was cultured in RPMI medium supplemented with 10% A⁺ human plasma (Hematology Center of University of Campinas) at 5% hematocrit in type O⁺ human red blood cells (Hematology Center of University of Campinas) and maintained at 37 $^\circ\text{C}$ in a 1% O_2 , 5% CO_2 , and 94% N_2 atmosphere, as described before.⁵³ Synchronous cultures were obtained from treatment with a 5% D-sorbitol (Sigma-Aldrich) solution. Test compound inhibition assays were performed as described previously.⁵⁴ Briefly, synchronized ring-stage (>90%) infected erythrocytes were dispensed in triplicate into 96-well plates (0.5% parasitemia and 2% hematocrit) in the presence of 50 μM of each crotofolane diterpenoid or the drug vehicle (DMSO), as a control. After 72 h of incubation, parasitemia was assessed by fluorometry using SybrGreen fluorescent dye. The growth inhibition

values were calculated on GraphPad Prism software and expressed as percentage relative to the drug-free control. The experiments were carried out in three independent assays.

Hemolysis Assay. The hemolysis assay was carried out according to Wang et al.⁵⁵ with some modifications. Suspensions of erythrocytes (2% hematocrit) were incubated with the test compounds at 50 μM of crotofolane diterpenoids or the drug vehicle (DMSO), as a control, at 37 $^\circ\text{C}$, 5% CO_2 , for 4 h. The reaction mixtures were centrifuged at 1000g for 5 min, and the absorbances of the supernatants were measured at 540 nm using a Biotek Synergy-HT spectrophotometer. The hemolytic rate was calculated in relation to the hemolysis of erythrocytes in 10% Triton X100 that was taken as 100%. The experiments were determined as in three independent assays.

■ ASSOCIATED CONTENT

Data Availability Statement

The original FIDs, NMR data files,^{56,57} and CSEARCH^{41,58,59} reports for compounds 1–6 are freely available on Zenodo with DOI: 10.5281/zenodo.6866841.

Supporting Information

The Supporting Information is available free of charge at <https://pubs.acs.org/doi/10.1021/acs.jnatprod.2c01007>.

NMR and MS data for the isolated compounds and antiviral, antibacterial, cytotoxicity, and antiplasmodial data (PDF)

X-ray crystallographic data for compound 1 (CIF)

■ AUTHOR INFORMATION

Corresponding Authors

Stephen S. Nyandoro – Chemistry Department, College of Natural and Applied Sciences, University of Dar es Salaam, 35061 Dar es Salaam, Tanzania; Email: nyandoro@udsm.ac.tz

Mate Erdelyi – Department of Chemistry – BMC, Uppsala University, SE-751 23 Uppsala, Sweden; orcid.org/0000-0003-0359-5970; Email: mate.erdelyi@kemi.uu.se

Authors

Emanuel T. Mahambo – Chemistry Department, College of Natural and Applied Sciences, University of Dar es Salaam, 35061 Dar es Salaam, Tanzania

Colores Uwamariya – Department of Infectious Diseases/Virology, Institute of Biomedicine, Sahlgrenska Academy, University of Gothenburg, S-413 46 Gothenburg, Sweden

Masum Miah – Department of Infectious Diseases/Virology, Institute of Biomedicine, Sahlgrenska Academy, University of Gothenburg, S-413 46 Gothenburg, Sweden

Leandro da Costa Clementino – Laboratory of Tropical Diseases - Prof. Dr. Luiz Jacinto da Silva, Department of Genetics, Evolution, Microbiology and Immunology, Institute of Biology (IB), University of Campinas - UNICAMP, Campinas 13083-970 SP, Brazil

Luis Carlos Salazar Alvarez – Laboratory of Tropical Diseases - Prof. Dr. Luiz Jacinto da Silva, Department of Genetics, Evolution, Microbiology and Immunology, Institute of Biology (IB), University of Campinas - UNICAMP, Campinas 13083-970 SP, Brazil

Gabriela Paula Di Santo Meztler – Department of Chemistry and Molecular Biology and Centre for Antibiotic Resistance Research (CARE), University of Gothenburg, SE-405 30 Gothenburg, Sweden

Edward Trybala – Department of Infectious Diseases/Virology, Institute of Biomedicine, Sahlgrenska Academy, University of Gothenburg, S-413 46 Gothenburg, Sweden

Joanna Said – Department of Infectious Diseases/Virology, Institute of Biomedicine, Sahlgrenska Academy, University of Gothenburg, S-413 46 Gothenburg, Sweden

Lianne H. E. Wieske – Department of Chemistry – BMC, Uppsala University, SE-751 23 Uppsala, Sweden; orcid.org/0000-0003-4617-7605

Jas S. Ward – Department of Chemistry, University of Jyväskylä, 40014 Jyväskylä, Finland; orcid.org/0000-0001-9089-9643

Kari Rissanen – Department of Chemistry, University of Jyväskylä, 40014 Jyväskylä, Finland; orcid.org/0000-0002-7282-8419

Joan J. E. Munissi – Chemistry Department, College of Natural and Applied Sciences, University of Dar es Salaam, 35061 Dar es Salaam, Tanzania

Fabio T. M. Costa – Laboratory of Tropical Diseases - Prof. Dr. Luiz Jacinto da Silva, Department of Genetics, Evolution, Microbiology and Immunology, Institute of Biology (IB), University of Campinas - UNICAMP, Campinas 13083-970 SP, Brazil

Per Sunnerhagen – Department of Chemistry and Molecular Biology and Centre for Antibiotic Resistance Research (CARE), University of Gothenburg, SE-405 30 Gothenburg, Sweden; orcid.org/0000-0002-0967-8729

Tomas Bergström – Department of Infectious Diseases/Virology, Institute of Biomedicine, Sahlgrenska Academy, University of Gothenburg, S-413 46 Gothenburg, Sweden

Complete contact information is available at:

<https://pubs.acs.org/10.1021/acs.jnatprod.2c01007>

Notes

The authors declare no competing financial interest.

ACKNOWLEDGMENTS

Financial support from the Swedish Research Council (2018-03918, 2019-03715), University of Dar es Salaam (CoNAS-CH 18035), and the São Paulo Research Foundation (FAPESP, grant 2017/18611-7), and the Center for Antibiotics Resistance Research (CARE) at the University of Gothenburg is highly appreciated. E.T.M. is thankful to UDSM for postgraduate studies sponsorship. This study made use of the NMR Uppsala infrastructure that is funded by the Department of Chemistry - BMC and the Disciplinary Domain of Medicine and Pharmacy. Mr. Frank Mbago (University of Dar es Salaam) is acknowledged for locating and identifying the plant species in the field, Katarzyna Palica (Uppsala University) for assistance with chiral compound HPLC separation, and Andreas Orthaber (Uppsala University) for initial X-ray diffraction experiments. L.C.C. and L.C.S.A. are grateful to the National Council for Scientific and Technological Development (CNPq), and G.P.D.S.M. is grateful to the Sven and Lilly Lawski Foundation for fellowships.

REFERENCES

- Salatino, A.; Salatino, M. L. F.; Negri, G. J. *Braz. Chem. Soc.* **2007**, *18*, 11–33.
- Wickens, G. E. *Flora of Tropical East Africa - Crassulaceae*; Royal Botanic Gardens: Kew, UK/CRC Press, Boca Raton, FL, 1987.
- Terefe, E. M.; Okalebo, F. A.; Derese, S.; Muriuki, J.; Mas-Claret, E.; Langat, M. K. *Nat. Prod. Res.* **2022**, *1*.
- Munissi, J. J. E.; Isyaka, S. M.; Mas-Claret, E.; Brabner, M.; Langat, M. K.; Nyandoro, S. S.; Mulholland, D. A. *Phytochemistry* **2020**, *179*, 112487.
- Xu, W.-H.; Liu, W.-Y.; Liang, Q. *Molecules* **2018**, *23*, 2333.
- Wu, X.-A.; Zhao, Y.-M.; Yu, N.-J. *J. Asian Nat. Prod. Res.* **2007**, *9*, 437–441.
- Zou, G.-A.; Su, Z.-H.; Zhang, H.-W.; Wang, Y.; Yang, J.-S.; Zou, Z.-M. *Molecules* **2010**, *15*, 1097–1102.
- Chávez, K.; Compagnone, R. S.; Riina, R.; Briceño, A.; González, T.; Squitieri, E.; Landaeta, C.; Soscún, H.; Suarez, A. I. *Nat. Prod. Commun.* **2013**, *8*, 1679–1682.
- Jogia, M. K.; Sinclair, A. R.; Andersen, R. J. *Oecologia* **1989**, *79*, 189–192.
- Kawakami, S.; Matsunami, K.; Otsuka, H.; Inagaki, M.; Takeda, Y.; Kawahata, M.; Yamaguchi, K. *Chem. Pharma. Bull.* **2015**, *63*, 1047–1054.
- Kawakami, S.; Toyoda, H.; Harinantenaina, L.; Matsunami, K.; Otsuka, H.; Shinzato, T.; Takeda, Y.; Kawahata, M.; Yamaguchi, K. *Chem. Pharma. Bull.* **2013**, *61*, 411–418.
- Kuo, P.-C.; Yang, M.-L.; Hwang, T.-L.; Lai, Y.-Y.; Li, Y.-C.; Thang, T. D.; Wu, T.-S. *J. Nat. Prod.* **2013**, *76*, 230–236.
- Ramos, F.; Takaishi, Y.; Kashiwada, Y.; Osorio, C.; Duque, C.; Acuña, R.; Fujimoto, Y. *Phytochemistry* **2008**, *69*, 2406–2410.
- He, R.; Zhang, Y.; Wu, L.; Nie, H.; Huang, Y.; Liu, B.; Deng, S.; Yang, R.; Huang, S.; Nong, Z.; Li, J.; Chen, H. *Phytochemistry* **2017**, *138*, 170–177.
- Song, J.-T.; Han, Y.; Wang, X.-L.; Shen, T.; Lou, H.-X.; Wang, X.-N. *Fitoterapia* **2015**, *107*, 54–59.
- Youngsa-ad, W.; Ngamrojanavanich, N.; Mahidol, C.; Ruchirawat, S.; Prawat, H.; Kittakoop, P. *Planta Med.* **2007**, *73*, 1491–1494.
- Athikomkulchai, S.; Prawat, H.; Thasana, N.; Ruangrunsi, N.; Ruchirawat, S. *Chem. Pharm. Bull.* **2006**, *54*, 262–264.
- Queiroz, M. M. F.; Queiroz, E. F. d.; Zeraik, M. L.; Marti, G.; Favre-Godal, Q.; Simões-Pires, C.; Marcourt, L.; Carrupt, P.-A.; Cuendet, M.; Paulo, M. *Phytochem. Lett.* **2014**, *10*, 88–93.
- Sun, Y.; Wang, M.; Ren, Q.; Li, S.; Xu, J.; Ohizumi, Y.; Xie, C.; Jin, D.-Q.; Guo, Y. *Fitoterapia* **2014**, *95*, 229–233.
- Radcliffe-Smith, A. *Kew Bull.* **1982**, *37*, 421–428.
- Tchissambou, L.; Chiaroni, A.; Riche, C.; Khuonghuu, F. *Tetrahedron* **1990**, *46*, 5199–5202.
- Kawakami, S.; Inagaki, M.; Matsunami, K.; Otsuka, H.; Kawahata, M.; Yamaguchi, K. *Chem. Pharm. Bull.* **2016**, *64*, 1492–1498.
- Piozzi, F.; Savona, G.; Hanson, J. R. *Phytochemistry* **1980**, *19*, 1237–1238.
- Burke, B. A.; Chan, W. R.; Pascoe, K. O.; Blount, J. F.; Manchand, P. S. *Tetrahedron Lett.* **1979**, *20*, 3345–3348.
- Silva, D. M.; Costa, E. V.; Nogueira, P. C. d. L.; Moraes, V. R. d. S.; Cavalcanti, S. C. d. H.; Salvador, M. J.; Ribeiro, L. H. G.; Gadelha, F. R.; Barison, A.; Ferreira, A. G. *Quim. Nova* **2012**, *35*, 1570–1576.
- Zhao, H.-Y.; Su, B.-J.; Zhou, W.-J.; Wang, Y.-Q.; Liao, H.-B.; Wang, H.-S.; Liang, D. *Bioorg. Chem.* **2020**, *105*, 104332.
- Etse, J. T.; Gray, A. I.; Waterman, P. G. *J. Nat. Prod.* **1987**, *50*, 979–983.
- Dutra, L. M.; Bomfim, L. M.; Rocha, S. L.; Nepel, A.; Soares, M. B.; Barison, A.; Costa, E. V.; Bezerra, D. P. *Bioorg. Med. Chem. Lett.* **2014**, *24*, 3315–3320.
- Haggag, M. I. *J. Bas. Environ. Sci.* **2021**, *8*, 91–96.
- Omokhua-Uyi, A. G.; Abdalla, M. A.; Leonard, C. M.; Aro, A.; Uyi, O. O.; Van Staden, J.; McGaw, L. J. *BMC Complement. Med. Ther.* **2020**, *20*, 1–15.
- Pabuprapap, W.; Wassanapit, Y.; Khetkam, P.; Chaichompo, W.; Kunkaewom, S.; Senabud, P.; Hata, J.; Chokchaisiri, R.; Svasti, S.; Suksamrarn, A. *Med. Chem. Res.* **2019**, *28*, 1755–1765.
- Yuan, Z.; Luan, G.; Wang, Z.; Hao, X.; Li, J.; Suo, Y.; Li, G.; Wang, H. *Chem. Biodivers.* **2017**, *14*, No. e1600487.
- Maeda, G.; van der Wal, J.; Gupta, A. K.; Munissi, J. J.; Orthaber, A.; Sunnerhagen, P.; Nyandoro, S. S.; Erdélyi, M. *J. Nat. Prod.* **2020**, *83*, 210–215.

- (34) Furukawa, M.; Makino, M.; Ohkoshi, E.; Uchiyama, T.; Fujimoto, Y. *Phytochemistry* **2011**, *72*, 2244–2252.
- (35) Kaewamatawong, R.; Ruangrunsi, N.; Likhitwitayawuid, K. *J. Nat. Med.* **2007**, *61*, 349–350.
- (36) Flack, H. D.; Bernardinelli, G. *J. Appl. Crystallogr.* **2000**, *33*, 1143–1148.
- (37) Parsons, S. *Tetrahedron-Asymmet* **2017**, *28*, 1304–1313.
- (38) Chan, W.; Prince, E.; Manchand, P.; Springer, J.; Clardy, J. *J. Am. Chem. Soc.* **1975**, *97*, 4437–4439.
- (39) Aldhafer, A.; Langat, M.; Ndunda, B.; Chirchir, D.; Midiwo, J. O.; Njue, A.; Schwikkard, S.; Carew, M.; Mulholland, D. *Phytochemistry* **2017**, *144*, 1–8.
- (40) Terefe, E. M.; Okalebo, F. A.; Derese, S.; Muriuki, J.; Rotich, W.; Mas-Claret, E.; Sadgrove, N.; Padilla-Gonzalez, G. F.; Prescott, T. A. K.; Siddique, H.; Langat, M. K. *J. Nat. Prod* **2022**, *85*, 1861–1866.
- (41) Robien, W. *Monatsh. Chem.* **2019**, *150*, 927–932.
- (42) Haber, E. A.; Kainulainen, K.; Van Ee, B. W.; Oyserman, B. O.; Berry, P. E. *Bot. J. Linn. Soc.* **2017**, *183*, 532–544.
- (43) Lopes, B. R. P.; da Costa, M. F.; Genova Ribeiro, A.; da Silva, T. F.; Lima, C. S.; Caruso, I. P.; de Araujo, G. C.; Kubo, L. H.; Iacovelli, F.; Falconi, M.; Desideri, A.; de Oliveira, J.; Regasini, L. O.; de Souza, F. P.; Toledo, K. A. *Virus Res.* **2020**, *276*, 197805.
- (44) Souza, M. R. P. d.; Ramos, A. V.; Oliveira, J. A. M. d.; Cabral, M. R.; Sampiron, E. G.; Scodro, R. B. d. L.; Foglio, M. A.; Ruiz, A. L. T.; Carmo, M. R. d.; Sarragiotto, M. H. *Nat. Prod. Res.* **2021**, *35*, 1–4.
- (45) Wellems, T. E.; Panton, L. J.; Gluzman, I. Y.; do Rosario, V. E.; Gwadz, R. W.; Walker-Jonah, A.; Krogstad, D. J. *Nature* **1990**, *345*, 253–255.
- (46) *CrysAlisPro Software System*, Oxford, UK, Rigaku Corporation, 2018.
- (47) Sheldrick, G. M. *Acta Crystallogr. A* **2015**, *71*, 3–8.
- (48) Dolomanov, O. V.; Bourhis, L. J.; Gildea, R. J.; Howard, J. A. K.; Puschmann, H. *J. Appl. Crystallogr.* **2009**, *42*, 339–341.
- (49) Mollel, J. T.; Said, J. S.; Masalu, R. J.; Hannoun, C.; Mbunde, M. V. N.; Nondo, R. S. O.; Bergstrom, T.; Trybala, E. *J. Ethnopharmacol* **2022**, *292*, 115204.
- (50) Lewis, F. A.; Rae, M. L.; Ferris, A. A.; Lehmann, N. I. *Med. J. Australia* **1961**, *2*, 932–933.
- (51) Mueller, J. H.; Hinton, J. P. *Soc. Exp. Biol. Med.* **1941**, *48*, 330–333.
- (52) Doyle, J. E.; Mehrhof, W. H.; Ernst, R. R. *Appl. Microbiol.* **1968**, *16*, 1742–1744.
- (53) Trager, W.; Jensen, J. B. *Science* **1976**, *193*, 673–5.
- (54) Hartwig, C. L.; Ahmed, A. O. A.; Cooper, R. A.; Stedman, T. T. In *Methods of Malaria Research*, 6 ed.; Moll, K.; Kaneko, A.; Scherf, A.; Wahlgren, M., Eds.; EVIMalaR: Glasgow, UK, 2013; pp 122–129.
- (55) Wang, C.; Qin, X.; Huang, B.; He, F.; Zeng, C. *Biochem. Biophys. Res. Commun.* **2010**, *402*, 773–777.
- (56) Kuhn, S.; Wieske, L. H. E.; Trevorrow, P.; Schober, D.; Schlorer, N. E.; Nuzillard, J. M.; Kessler, P.; Junker, J.; Herraes, A.; Fares, C.; Erdelyi, M.; Jeannerat, D. *Magn. Reson. Chem.* **2021**, *59*, 792–803.
- (57) Pupier, M.; Nuzillard, J. M.; Wist, J.; Schlorer, N. E.; Kuhn, S.; Erdelyi, M.; Steinbeck, C.; Williams, A. J.; Butts, C.; Claridge, T. D. W.; Mikhova, B.; Robien, W.; Dashti, H.; Eghbalian, H. R.; Fares, C.; Adam, C.; Kessler, P.; Moriaud, F.; Elyashberg, M.; Argyropoulos, D.; Perez, M.; Giraudeau, P.; Gil, R. R.; Trevorrow, P.; Jeannerat, D. *Magn. Reson. Chem.* **2018**, *56*, 703–715.
- (58) Robien, W. *Planta Med.* **2019**, *85*, 1414–1414.
- (59) Kalchauer, H.; Robien, W. *J. Chem. Inf. Comp. Sci.* **1985**, *25*, 103–108.